Analysis of two-particle transfer reaction in the ^{18}O+^{40}Ca and ^{20}Ne+^{116}Cd collisions

J. L. Ferreira[1] and J. Lubian[1] and E. N. Cardozo[1] and F. Cappuzzello[2,3] and M. Cavallaro[2] and D. Carbone[2] for the NUMEN collaboration

[1]Instituto de Física, Universidade Federal Fluminense, Niterói, Rio de Janeiro, 24210-340, Brazil
[2]Istituto Nazionale di Fisica Nucleare - Laboratori Nazionali del Sud, via S. Sofia 62, 95123, Catania, Italy
[3]Dipartimento di Fisica e Astronomia "Ettore Majorana", University of Catania, via Santa Sofia 64, 95123, Catania, Italy

E-mail: jonasleonardo@id.uff.br

Abstract. Two-neutron and two-proton transfer reactions have been analyzed in the present work. These kind of transfer reactions is an excellent tool to get insights into the short-range correlations on nucleons in a nuclear state. The direct and sequential two-particle transfer mechanisms, for which the valence particles can be transferred, were compared one with other to probe the populated nuclear states. Large-scale shell model calculations were performed to obtained the spectroscopic amplitudes for one and two valence particles.

1. Introduction

Two-nucleon transfer reactions are very good tools to investigate two-nucleon correlations in nuclear states. In the last years, such reactions have extensively been studied by considering the reactions such as (p,t)[1], (^{16}O,^{14}C)[2, 3, 4], (^{18}O, ^{16}O) [5, 6, 7, 8, 9, 10, 11], (^{20}Ne, ^{18}O)[12] and (^{18}O, ^{20}Ne) [13]. A complete treatment of the two-nucleon transfer reactions needs to include explicitly the inelastic excitations and evaluate the contributions of the direct and sequential mechanisms. So, a relevant nuclear structure information concerning the partners of the collision is represented by the spectroscopic amplitudes, which can be derived from different structure model such as, for instance, large-scale shell model calculation. In this way, the nuclear structure and the dynamic of the reactions are combined to assess microscopically the role of the simultaneous and sequential mechanisms in two-nucleon transfer reactions. Some of the studied cases, the theoretical predictions showed that the simultaneous process is dominant over the sequential one by populating the ground state in the final partition. In others cases the collectivity of the populated state by the two transferred nucleons has favoured the sequential mechanism over the direct process [9, 14].

In particular, reactions in which double charge exchange (DCE) take place, such as (^{20}Ne, ^{20}O) and (^{18}O, ^{18}Ne), have gained attention because they can provide information about the inverse double-beta decay process [15, 16]. The NURE[17] and NUMEN[18] projects proposed a comprehensive study of the experimental data and theoretical predictions concerning the nuclear matrix elements associated to the exchange of two correlated isovector mesons, between projectile

and target, in DCE reactions. This class of direct reactions might be used as surrogate to the hypothetical neutrinoless double beta decay ($0\nu\beta\beta$) phenomenon. On the other hand, once the double charge exchange reaction can occur by nucleons or mesons exchange between projectile and target, which are two completely different processes, it is important to know the relevance of the multinucleon transfer mechanism in DCE reactions. The analysis of these reactions also offer an opportunity to study and learn about the nuclear structure properties of the states accessed by mean of two-particle transfer processes, as for instance in ^{116}Cd(^{20}Ne, ^{18}O)^{118}Sn and ^{116}Cd(^{20}Ne,^{22}Ne)^{114}Cd or in ^{40}Ca(^{18}O,^{20}Ne)^{38}Ar reactions. Moreover, the good description of the experimental data by the theoretical model can provide precise prediction about the cross sections of the multinucleon transfer in DCE process (TDCE).

In the present work, we show some recent results for the cross sections corresponding to the two-particle transfer in the ^{18}O+^{40}Ca and ^{20}Ne+^{116}Cd collisions at, respectively, 270 MeV and 306 MeV incident energies. The relevance of the direct and sequential two-particle mechanisms from which both transferred particles populate the final channels is discussed. Large-scale shell model calculations are carried out to determine the spectroscopic amplitudes for one- and two-particle concerning the projectile and target overlaps.

2. Results and discussion

In present analysis, we have evaluated two-particle transfer cross section for the ^{18}O+^{40}Ca and ^{20}Ne+^{116}Cd collisions. In particular, we have an interesting case for two-proton transfer in both of these collisions. For the targets side, both transferred proton are removed from a closed shell in ^{40}Ca nucleus or added to complete the shell in ^{116}Cd target.

2.1. Two-proton pickup transfer in the ^{18}O+^{40}Ca collision at 270 incident energy.

In nuclear collisions, two particles can be transferred from a simultaneous process or from a sequential two step mechanism in which an intermediate partition is formed. In the direct mechanism, the coupled reaction channel (CRC) method is used by considering the independent coordinates scheme to determine the cross sections for the desired channels. The single particle wave functions of each valence nucleon are constructed by Woods-Saxon potentials. The depths of these potentials are varied to fit the experimental one-nucleon separation energies. Then a transformation of coordinates is performed to convert the independent coordinates of both valence nucleons into the center of mass coordinates of the two nucleons and the relative motion coordinate. This methodology has extensively been used in Refs.[5, 8, 9, 12, 13, 14, 19, 20]. To perform the transfer calculations the FRESCO code [21, 22] is used to solve the coupled reaction Schrödinger equations. Conversely, the distorted wave Born approximation (DWBA) or coupled channel Born Approximation (CCBA) methods is considered when both valence particles are transferred sequentially. In these transfer calculations, the optical potentials are built with the double folding São Paulo potential [23, 24] for which the imaginary part is assumed to be equal to the real part multiplied by a factor strength so that $W(R) = NV(R)$. With $V(R) = V_{LE}^{SP}(R) \times e^{4v^2/c^2}$ and N being the coefficient strength factor. In analysis of elastic scattering cross sections for many systems, a coefficient $N = 0.78$ [23, 25, 26] has been able to describe the experimental data in the one-channel calculations approach. Pereira et al. [27] has shown that a reduced coefficient strength $N = 0.60$ should be used for the imaginary part of the optical potential, since the couplings with relevant inelastic states are included explicitly in the coupled equations scheme. Many systems have been analyzed by considering this methodology in two-particle transfer reaction ^{18}O+^{12}C[5],^{18}O+^{13}C[8], ^{18}O+^{16}O[6, 7, 28], ^{18}O+^{28}Si[9, 28], ^{18}O+^{64}Ni[14, 28], ^{20}Ne+^{116}Cd[12, 29], ^{9}Be+^{7}Be[19], d+^{55}Mn[30], ^{18}O+^{40}Ca[31] and ^{18}O+^{48}Ti[32].

The spectroscopic amplitudes for the one- and two-particle valence are determined with structure shell model calculations by using the NUSHELLX [33] code. The ZBM effective

interaction [34] was considered in the shell model Hamiltonian for the projectile overlaps. This interaction was elaborated by considering a ^{12}C nucleus as closed core and the $1p_{1/2}$, $1d_{5/2}$, and $2s_{1/2}$ as valence orbits for both neutrons and protons. For the target overlaps, a model space represented by the $2s_{1/2}$, $1d_{3/2}$, $1f_{7/2}$, and $2p_{3/2}$ valence orbits for protons and neutrons has been assumed. The phenomenological shell model ZBM*mod* interaction was used, in which was built from a modification of the Windenthal [35] and Kuo-Brown interactions [36, 37].

In Fig. 1, we first present the angular distributions obtained for two-proton transfer in the ^{40}Ca(^{18}O,^{20}Ne)^{38}Ar reaction at 270 MeV incident energy. The left panel corresponds to the channel in which the ejectile and residual nuclei stand in their ground states. In the right panel, the angular distribution corresponds to the experimental excitation energy with peak in 1.8 MeV (see Fig.1 in [13]). So, the experimental angular distribution contains the contribution of two channels identify as ^{20}Ne$_{g.s.}$+^{38}Ar$_{2.168}$ or ^{20}Ne$_{1.634}$+^{38}Ar$_{g.s.}$, once the experimental energy resolution was 500 keV [13]. The coupling scheme and spectroscopic amplitudes for one- and two-proton transfer used in the transfer calculations can be obtained in Ref. [13]. As one can observe in this figure, the theoretical descriptions of the experimental data are quite well. Besides, in right panel we can realize two interesting feature of the theoretical results. First, the sequential mechanism for the two-particle transfer dominate over the direct one when the angle increase. Second, the more relevant channel is that in which the ^{20}Ne nucleus is found in its 2^+ excited state. The high collectivity of this excited state favours the sequential mechanism to populated it. This kind of behavior has also been observed in the two-neutron stripping transfer in the ^{18}O+^{28}Si and ^{18}O+^{64}Ni collisions [9, 14]. The full black line represent the coherent sum between the direct and sequential mechanisms, once both can be present during the reaction.

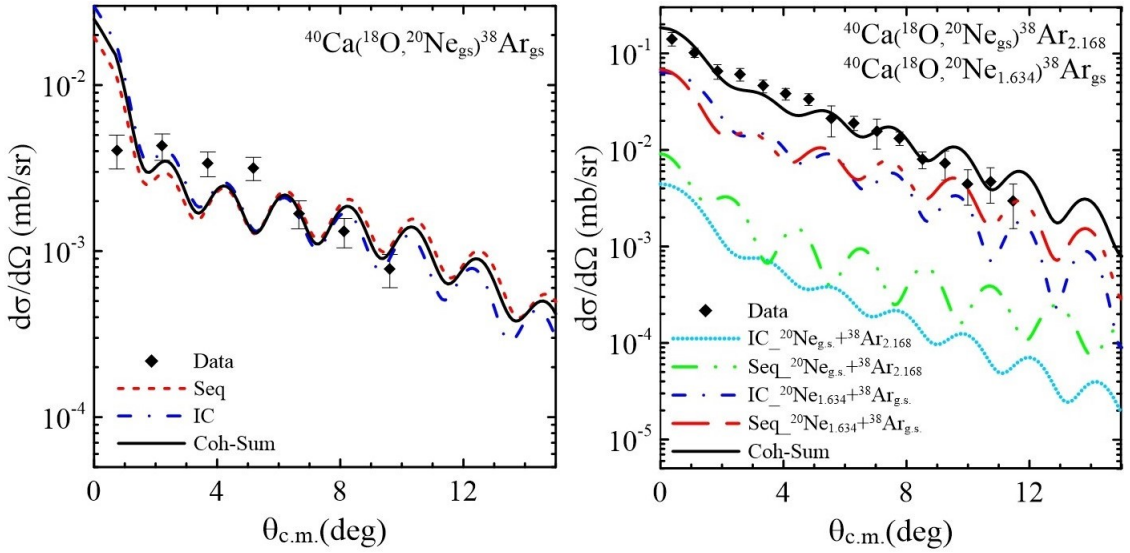

Figure 1. (color online) Comparison between the theoretical and experimental two-proton transfer angular distribution corresponding to: (left panel) the ^{20}Ne$_{gs}(0^+)+^{38}$Ar$_{gs}(0^+)$ channel; (right panel) unresolved excited states concerning the second peak in Fig. 1 from Ref. [13]. In both figures the contribution due to the simultaneous (IC) and sequential (Seq) transfer and the coherent (Coh) sum of the two mechanisms are shown.

2.2. Two-proton stripping transfer in the ^{20}Ne+^{116}Cd collision at 306 incident energy.
Here, the same methodology used in previous subsection was employed to calculate the two-proton and two-neutron transfer cross sections in the reaction ^{116}Cd(^{20}Ne,^{18}O)^{118}Sn and

^{116}Cd(^{20}Ne,^{22}Ne)^{114}Cd reactions, respectively. The spectroscopic amplitude for the projectile overlaps were obtained by considering a larger model space in the structure shell model calculation than that used in the previous subsection. So, the *psdmod* interactions was considered in the shell model Hamiltonian for which the full *p-sd* model is considered. Despite this difference, the spectroscopic amplitudes obtained for the projectile overlaps were similar to those one obtained with the ZBM interaction (see Refs. [12, 13]). For the target overlap, the spectroscopic amplitudes were calculated by considering two different proton model space. In the first case, we considered the proton valence space as composed by the orbits $1f_{5/2}$, $2p_{3/2}$, $2p_{1/2}$ and $1g_{9/2}$. In the second case, the orbits $2p_{1/2}$, $1g_{9/2}$, $1g_{7/2}$ and $2d_{5/2}$ were considered as valence space for the protons. In this way, it was possible to probe the importance of the orbits above the full closed shell pf-$g_{9/2}$ by populating the eigenstates of the ^{118}Sn residual nucleus in the final partition. The neutron model space in both of the cases was the same. It was formed by the $1g_{7/2}$, $2d_{5/2}$, $2d_{3/2}$, $3s_{1/2}$ and $1h_{11/2}$ orbits. The correspondent effective interaction used in the structure shell model calculations for the target overlaps were, respectively, the called $jj45pna$[38] and $88Sr45$[39] interactions, which are based in CD-bonn[40, 41] nucleon-nucleon interactions. The $1h_{11/2}$ was considered to be closed by limited computational capability. All the spectroscopic amplitudes for both projectile and target overlaps can be obtained in the supplemental material of Ref. [12].

Table 1. Comparison between the experimental and theoretical cross sections for the two-neutron transfer reactions ^{116}Cd(^{20}Ne,^{22}Ne)^{114}Cd, integrated in $4.5° \leq \theta \leq 14.5°$, and two-proton transfer reaction ^{116}Cd(^{20}Ne,^{18}O)^{118}Sn, integrated in $4° \leq \theta \leq 14°$.

	Cross Sections (nb) for two-neutron transfer				
Final channel	Exp.	SA (psdmod+jj45pna)			
		IC	Seq		
^{22}Ne$_{g.s.}(0^+)$+^{116}Cd$_{g.s.}(0^+)$	370 ± 190	209	427		
^{22}Ne$_{g.s.}(0^+)$+^{116}Cd$_{0.558}(2^+)$	420 ± 190	314	636		
	Cross Sections (nb) for two-proton transfer				
Final channel	Exp.	SA (psdmod+jj45pna)		SA (psdmod+88Sr45)	
		IC	Seq	IC	Seq
^{18}O$_{g.s.}(0^+)$+^{118}Sn$_{g.s.}(0^+)$	40 ± 15	30.9	52.1	39.5	88.5
^{18}O$_{g.s.}(0^+)$+^{118}Cd$_{1.229}(2^+)$	140 ± 60	26.9	39.8	52.7	106.3

In Table 2.2, the results for the two-neutron and two-proton transfer cross sections are presented. For the two-neutron transfer, from a pickup reaction, the theoretical cross sections could describe quite well the experimental data. The spectroscopic amplitudes for the target overlaps were obtained with the $jj45pna$ interaction in the shell model calculation. Both of the measured channel were quite well described. On the other hand, this not completely true for the two-proton transfer from a stripping reaction by using the $jj45pna$ spectroscopic amplitudes. Only the integrated cross section for the ^{18}O$_{g.s.}(0^+)$+^{118}Sn$_{g.s.}(0^+)$ channel was well described. As one can observe in this table, the cross section for the channel ^{18}O$_{g.s.}(0^+)$+^{118}Sn$_{1.229}(2^+)$ is underestimated by the calculations by a factor around 4. To verify the influence of the model space used in the transfer CRC calculations, we performed the structure calculation to obtain the spectroscopic amplitudes for the target overlaps by using the effective $88Sr45$ interaction. In this way, we can see the influence of the orbits $1g_{7/2}$ and $2d_{5/2}$ in the transfer mechanism. In Table 2.2, one realize that the results for the ^{18}O$_{g.s.}(0^+)$+^{118}Sn$_{1.229}(2^+)$ channel was improved in which the sequential two-proton transfer was able to describe the experimental cross section.

This shows the relevance of the model space used in the dynamic of the transfer reaction, in which the orbits $1g_{7/2}$ and $2d_{5/2}$ play a important role in the description of the cross section populating the $^{18}O_{g.s.}(0^+)+^{118}Sn_{1.229}(2^+)$ channel .

3. Conclusion

This work has presented cross sections for specific channels corresponding to the two-particle transfer in the $^{40}Ca(^{18}O,^{20}Ne)^{38}Ar$, $^{116}Cd(^{20}Ne,^{22}Ne)^{114}Cd$ and $^{116}Cd(^{20}Ne,^{18}O)^{118}Sn$ reactions. The experiments were performed at the INFN-LNS laboratory in Catania in the framework of the NUMEN project where the K800 Superconducting Cyclotron beam has accelerated the $^{18}O^{4+}$ beam at 270 MeV incident energy in the $^{18}O+^{40}Ca$ collision, and $^{20}Ne^{4+}$ beam at 306 MeV incident energy in the $^{20}Ne+^{116}Cd$ collision.

In both $^{18}O+^{40}Ca$ and $^{20}Ne+^{116}Cd$ collisions, the complete study of the reaction mechanism and nuclear structure issues has been performed. These heavy ions reactions provide an interesting experimental tool to probe the nuclear matrix elements corresponding to the double-charge exchange reactions[12, 13].

From the theoretical analysis, the direct and sequential two-particle transfer mechanisms were evaluated considering finite-range coupled reaction channel (CRC) and coupled-channel Born approximation (CCBA) methods, respectively. In the $^{40}Ca(^{18}O,^{20}Ne)^{38}Ar$ reaction, for instance, the channel $^{20}Ne_{g.s.}(0^+)+^{40}Ca_{g.s.}(0^+)$ was populated with similar strength by the direct and sequential processes. On the other hand, the channels $^{20}Ne_{g.s.}(0^+)+^{38}Ar_{2.168}(2^+)$ and $^{20}Ne_{1.634}(2^+)+^{38}Ar_{g.s.}(0^+)$ have been, preferably, populated through the sequential process. This behaviour was also observed in two-proton transfer populating the first excited state of the $^{118}Sn_{1.23}(2^+)$ in the $^{116}Cd(^{20}Ne,^{18}O)^{118}Sn$ reaction. Moreover, for the two-neutron transfer, in the $^{116}Cd(^{20}Ne,^{22}Ne)^{114}Cd$ reaction, the competition between direct and sequential mechanisms by populating both channels $^{22}Ne_{g.s.}(0^+)+^{114}Cd_{g.s.}(0^+)$ and $^{22}Ne_{g.s.}(0^+)+^{114}Cd_{0.558}(2^+)$ was observed.

From the structure calculation side, the spectroscopic amplitudes for the projectile and target overlaps were derived from the microscopic large-scale shell model calculations. In particular, for the $^{116}Cd(^{20}Ne,^{18}O)^{118}Sn$ reaction, two different model spaces for the valence protons were taken into account in the effective shell model Hamiltonian to verify the influence of the proton valence space in the dynamic of reaction.

All these results have an important application in the analysis of double charge exchange reactions, once both the two-particle transfer reactions, studied in this paper, represent the first step (direct two-particle process) or first two steps (sequential two-particle process) in the peripheral multinucleon transfer reactions that might compete with the hypothetical direct meson exchange mechanism in the $^{40}Ca(^{18}O,^{18}Ne)^{40}Ar$ and $^{116}Cd(^{20}Ne,^{20}O)^{116}Sn$ reactions.

The satisfactory description of the experimental data indicate that the microscopic treatment of the approach used in the current work could be safely used to predict the cross sections concerning the multinucleon transfer process, for which the double charge exchange (DCE) reaction is measured. This is a confirmation of the validity of the approach used for the two-neutron and two-proton transfer reactions studied in this work.

Acknowledgment

The Brazilian authors acknowledge partial financial support from CNPq, FAPERJ, CAPES and INCT-FNA (Instituto Nacional de Ciência e Tecnologia- Física Nuclear e Aplicações) research project 464898/2014-5.

References

[1] Potel G, Barranco F, Marini F, Idini A, Vigezzi E and Broglia R A 2011 *Phys. Rev. Lett.* **107**(9) 092501
[2] Tamura T, Low K and Udagawa T 1974 *Physics Letters B* **51** 116–118 ISSN 0370-2693

[3] Lemaire M C, Mermaz M C, Sztark H and Cunsolo A 1974 *Phys. Rev. C* **10**
[4] Jha V, Roy B, Chatterjee A, Patel H, Srinivasan B, Betigeri M and Machner H 2002 *Eur. Phys. J. A* **15** 389–397 ISSN 1434-601X
[5] Cavallaro M, Cappuzzello F, Bondì M, Carbone D, Garcia V N, Gargano A, Lenzi S M, Lubian J, Agodi C, Azaiez F, De Napoli M, Foti A, Franchoo S, Linares R, Nicolosi D, Niikura M, Scarpaci J A and Tropea S 2013 *Phys. Rev. C* **88**(5) 054601
[6] Ermamatov M J, Cappuzzello F, Lubian J, Cubero M, Agodi C, Carbone D, Cavallaro M, Ferreira J L, Foti A *et al.* 2016 *Phys. Rev. C* **94** 024610
[7] Ermamatov M J *et al.* 2017 *Phys. Rev. C* **96** 044603
[8] Carbone D *et al.* 2017 *Phys. Rev. C* **95** 034603
[9] Cardozo E N, Lubian J, Linares R, Cappuzzello F, Carbone D, Cavallaro M, Ferreira J L, Gargano A, Paes B and Santagati G 2018 *Phys. Rev. C* **97**(6) 064611
[10] Cappuzzello F, Carbone D, Cavallaro M, Spatafora A, Ferreira J, Agodi C, Linares R and Lubian J 2021 *Eur. Phys. J. A* **57** 34
[11] Cappuzzello F, Carbone D, Cavallaro M, Bondì M, Agodi C, Azaiez F, Bonaccorso A, Cunsolo A, Fortunato L, Foti A, Franchoo S, Khan E, Linares R, Lubian J, Scarpaci J and Vitturi A 2015 *Nature Communications* **6** 6743
[12] Carbone, D and Ferreira, JL and Calabrese, S and Cappuzzello, F and Cavallaro, M and Hacisalihoglu, A and Lenske, H and Lubian, J and Magaña Vsevolodovna, RI and Santopinto, E and Agodi, and others (for the NUMEN Collaboration) 2020 *Phys. Rev. C* **102** 044606
[13] Ferreira, J L and Carbone, D and Cavallaro, M and Deshmukh, NN and Agodi, C and Brischetto, GA and Calabrese, S and Cappuzzello, F and Cardozo, EN and Ciraldo, I and Cutuli, M and Fisichella, M and Foti, A and La Fauci, L and Sgouros, O and Soukeras, V and Spatafora, A and Torresi, D and Lubian, J (for the NUMEN Collaboration) 2021 *Phys. Rev. C* **103** 054604
[14] Paes B *et al.* 2017 *Phys. Rev. C* **96** 044612
[15] Lenske H, Bellone J, Colonna M and Gambacurta D 2021 *Universe* **7** 98
[16] Lenske H 2018 *J. Phys. Conf. Ser.* **1056** 012030
[17] Cavallaro M *et al.* 2017 *Proceedings of Science* **BORMIO2017** 015
[18] Cappuzzello F, Agodi C, Cavallaro M, Carbone D, Tudisco S, Lo Presti D, Oliveira J, Finocchiaro P, Colonna M, Rifuggiato D, Calabretta L, Calvo D *et al.* 2018 *Eur. Phys. J. A* **54** 72
[19] Umbelino, U and Pires, K C C and Lichtenthäler, R and Scarduelli, V and Scotton, G A and Lépine-Szily, A and Guimaraes, V and Lubian, J and Paes, B and Ferreira, J L and Alvarez, M A G and Shorto, J M B and Appannababu, S and Assunçao, M and Condori, R P and Morcelle, V 2019 *Phys. Rev. C* **99**(6) 064617
[20] Ferreira, J L and Lubian, J and Cappuzzello, F and Cavallaro, M and Carbone, D (NUMEN Collaboration) 2022 *Phys. Rev. C* **105**(1) 014630
[21] Thompson I J *http://www.fresco.org.uk*
[22] Thompson I J 1988 *Comput. Phys. Rep.* **7** 167 – 212
[23] Chamon L C, Carlson B V, Gasques L R, Pereira D, De Conti C, Alvarez M A G, Hussein M S, Candido Ribeiro M A, Rossi Jr E S and Silva C P 2002 *Phys. Rev.* **C66** 014610
[24] Chamon L C, Carlson B V, Gasques L R, Pereira D, De Conti C, Alvarez M A G, Hussein M S, Cândido Ribeiro M A, Rossi E S and Silva C P 2002 *Phys. Rev. C* **66**(1) 014610
[25] Gasques L, Chamon L, Gomes P and Lubian J 2006 *Nucl. Phys. A* **764** 135–148
[26] Alvarez M, Chamon L, Hussein M, Pereira D, Gasques L, Rossi E and Silva C 2003 *Nucl. Phys. A* **723** 93 – 103
[27] Pereira D, Lubian J, Oliveira J R B, de Sousa D P and Chamon L C 2009 *Phys. Lett. B* **670** 330 – 335
[28] Linares R, Ermamatov M J, Lubian J, Cappuzzello F, Carbone D, Cardozo E N, Cavallaro M, Ferreira J L, Foti A, Gargano A, Paes B, Santagati G and Zagatto V A B 2018 *Phys. Rev. C* **98**(5) 054615
[29] Burrello S *et al.* 2022 *Phys. Rev. C* **105** 024616
[30] Cardozo E N, Ermamatov M J, Ferreira J L, Paes B, Sinha M and Lubian J 2018 *Eur. Phys. J. A* **54**(9) 150
[31] Calabrese S, Cavallaro M, Carbone D, Cappuzzello F, Agodi C, Burrello S, De Gregorio G, Ferreira J L, Gargano A, Sgouros O, Acosta L, Amador-Valenzuela P, Bellone J I *et al.* (NUMEN Collaboration) 2021 *Phys. Rev. C* **104**(6) 064609
[32] Sgouros O, Cavallaro M, Cappuzzello F, Carbone D, Agodi C, Gargano A, De Gregorio G, Altana C, Brischetto G A, Burrello S, Calabrese S, Calvo D *et al.* (for the NUMEN Collaboration) 2021 *Phys. Rev. C* **104**(3) 034617
[33] *NuShell for Windows and Linux, http://www.garsington.eclipse.co.uk/*
[34] Zuker A P, Buck B and McGrory J B 1968 *Phys. Rev. Lett.* **21**(1) 39–43
[35] Wildenthal B 1984 *Progress in Particle and Nuclear Physics* **11** 5–51

[36] Poves A and Zuker A 1981 *Physics Reports* **70** 235–314
[37] Kahana S, Lee H C and Scott C K 1969 *Phys. Rev.* **180**(4) 956–966
[38] Machleidt R 2001 *Phys. Rev. C* **63**(2) 024001
[39] Coraggio L, Gargano A and Itaco N 2016 *Phys. Rev. C* **93**(6) 064328
[40] Machleidt R, Holinde K and Elster C 1987 *Physics Reports* **149** 1–89
[41] Machleidt R 1989 *The Meson Theory of Nuclear Forces and Nuclear Structure* (Boston, MA: Springer US) pp 189–376